Available online at www.sciencedirect.com
SCIENCE DIRECT
Polymer 46 (2005) 4882–4890
polymer
www.elsevier.com/locate/polymer

Single and mixed gas diffusion through polyethylene films

M. Pino, R.A. Duckett, I.M. Ward*

IRC in Polymer Science and Technology, School of Physics and Astronomy, University of Leeds, Leeds LS2 9JT, UK

Received 17 December 2004; received in revised form 3 February 2005; accepted 4 February 2005
Available online 19 April 2005

Abstract

In this paper, the results of using a mass spectrometer technique to measure mixed-gas diffusion through polymer films are presented. Mixtures of oxygen, carbon dioxide and nitrogen are diffused through films of polyethylene with different degrees and type of chain branching. It is shown that in the case of pure gases Henry's law applies; the gas concentration is proportional to the partial pressure of gas. It is also demonstrated that there is a reasonable correlation between gas solubilities and the Lennard–Jones force constants, although detailed departures from this behaviour are observed for the different materials.

The results show that, in general, the presence of one gas can affect the diffusion and solubility of another, although the solubility and diffusion of carbon dioxide were found to be independent of other gases. In particular, an apparent competition is observed between nitrogen and oxygen in terms of solubility. Moreover, the nature of the interaction between gases depends on the degree of branching and the state of annealing of the polyethylene. Contrary to expectation, it is shown that annealing, whilst increasing the crystallinity, increases the permeability of all gases for the only two samples studied in this regard.

Keywords: Permeability; Mixed gases; Polyethylene

1. Introduction

Although there have been extensive studies of the relative permeabilities of mixed gases in permeable membranes, for example [1–3] because of the development of methods for gas separation, much less is known regarding the diffusion and solubility of gas mixtures in low permeability polymer films. In a previous paper [4], two of the present authors describe results for diffusion and solubility of mixtures of oxygen (O_2), nitrogen (N_2) and carbon dioxide (CO_2) in polyethylene terephthalate films. It was found that the behaviour of one gas could be significantly affected by the presence of a second gas and that the details of such effects were modified by the polymer structure with considerable differences, for example, between amorphous and biaxially oriented films. Similar results have recently been reported for oxygen/water mixtures in polylactide films, by Auras and co-workers [5].

In this paper, results are presented for O_2, N_2 and CO_2 mixtures in several polyethylene films of different chemical composition; specifically in terms of degree and nature of branching. These results show that the magnitude of any effects relating to the behaviour of gas mixtures depends significantly on subtle details of the chemical composition, as well as the morphology. It will be shown, for example, that the behaviour does not depend only on the degree of crystallinity, as has often been previously supposed, but on specific features of the polymer morphology, which are very dependent on the preparation of the films, including any annealing treatment.

2. Theory

The gas transport properties through polymers can be described by three parameters, the diffusion coefficient, the permeability coefficient, and the solubility. These terms are interrelated although the precise nature of the correlation is dependant on the type of diffusion which occurs. In this case the Fickian diffusion was assumed. These properties can be determined either from the absorption experiment or from

* Corresponding author. Tel.: +44 113 343 3808; fax: +44 113 343 3809.
E-mail address: i.m.ward@leeds.ac.uk (I.M. Ward).

0032-3861/$ - see front matter © 2005 Elsevier Ltd. All rights reserved.
doi:10.1016/j.polymer.2005.02.118

Table 1
Characteristics of polyethylene materials

Polymer	Grade	Density (kg/m^3)	M_w	M_w/M_n	Short chain branch content/1000 °C
LDPE	LD5310AA	0.921	100,000	7	~30
LLDPE	LL6208AF	0.920	150,000	4.6	~16
HDPE	Hizex 7000F	0.942	315,000	21	~2

the desorption experiment, which is further explained in detail.

The diffusion is the speed with which a gas molecule penetrates through the polymer. The diffusion coefficient, D, is based on Fick's first law of diffusion. It states that the flux in the x direction F is proportional to the concentration gradient ($\partial c/\partial x$).

$$F = -D\left(\frac{\partial c}{\partial x}\right) \tag{1}$$

The flux, F, is the volume of substance diffusing across unit area in unit time, independent of the state of aggregation of the polymer. This first law is applicable to diffusion in the steady state, that is, where concentration is not varying with time.

The change in concentration with the time at a distance x into a thin sheet, where the flux is in the x direction only, is given by

$$\frac{\partial c}{\partial t} = -\frac{\partial F_x}{\partial x} \tag{2}$$

and so from Eq. (1), we have

$$\frac{\partial c}{\partial t} = \frac{\partial}{\partial x}\left(D\frac{\partial c}{\partial x}\right) \tag{3}$$

If D is independent of concentration, the Eq. (3) can be written as

$$\frac{\partial c}{\partial t} = D\frac{\partial^2 c}{\partial x^2} \tag{4}$$

The geometry of the film must be such that diffusion into the edges can be neglected. Eq. (4) can be solved to provide an expression for the flux passing through a film.

$$\Delta F = \left[(4/\sqrt{\pi})X\sum_{i=1}^{\infty}\exp(-n_i^2X^2)\right]\Delta F_\infty \quad \text{for } n \text{ odd} \tag{5}$$

Here ΔF is the flux above background level, ΔF_∞ is the final steady-state flux above background, $X^2 = l^2/(4Dt)$, where l is the sample thickness, t is the time after the gas was admitted. This solution has a sigmoidal shape.

The permeability coefficient, P, concerns the steady-state flux, F, of gas passing through the polymer and the pressure difference across it which gives the driving force:

$$F = P\frac{(p_1 - p_2)}{l} \tag{6}$$

where p_1 and p_2 are the partial pressures on opposite sides of a film of thickness l. P is expressed in cubic centimetres of gas at STP per square centimetre of film one centimetre thick per second for a pressure difference of one centimetre of mercury.

The solubility, S, is defined as the amount of dissolved gas in the polymer divided by the volume of the sample for 1 atm of gas on the sample surface

$$\begin{aligned} &(c_1 - c_2) = S(p_1 - p_2), && \text{and } p_2 \approx 0, \quad c_2 \approx 0 \\ &c_1 = Sp_1, && \text{and } p_1 = 1 \text{ atm} \\ &S = \frac{c_1}{p_1}, && \text{and } p_1 = 1 \text{ atm} \end{aligned} \tag{7}$$

where c_1 is the concentration in the sample when the equilibrium is reached. Eq. (7) obeys Henry's law when S is independent of p, and hence Eqs. (1), (6) and (7)) can be written as

$$S = 76\frac{P}{D} \tag{8}$$

The solubility is expressed in cubic centimetres of gas at STP per cubic centimetres of the solid at a pressure of 76 cm of mercury, which is atmospheric pressure.[1]

3. Experimental section

3.1. Materials

Three commercial grades of polyethylene were studied, a low density polyethylene (LDPE); LD 5310 AA, a linear low density polyethylene (LLDPE), LL 6208 AF and a high density polyethylene (HDPE), Hizex 7000F. The LDPE and LLDPE polymers were supplied by BP Chemicals and the HDPE by Mitsui Chemicals, Japan. The characterisation of these materials are summarised in Table 1.

The LDPE was produced by the ICI high pressure process. It contains a distribution of short chain branches (ethyl, butyl, amyl, etc.) and the long chain branching characteristic of free radical polymerisation. The LLDPE is a copolymer of ethylene and hexene-1, with a branch distribution characteristic of Ziegler polymerisation with a wide range of short chain branches from less than five to greater than 25 branches/1000 carbon atoms. The HDPE is

[1] N.B. It is conventional to write $P = DS$ when the units of P and S are chosen appropriately.

Table 2
Compression moulding conditions

Sample	Starting material	Mould temperature (°C)	Mould pressure (psi)	Moulding time (min)	Cooling procedure
LDPE	Polymer sheets	160	60	40	Slow cooled in mould
LLDPE	Polymer pellets	170	500	5	Quenched into cold water
HDPE	Polymer pellets	155	500	5	Quenched into cold water

an ethylene–butane copolymer with only 2-ethyl branches/1000 carbon atoms.

3.2. Sample preparation

Isotropic polymer sheets were produced by compression moulding in a hydraulic press. These are designated LDPE, LLDPE and HDPE; the production conditions are summarised in Table 2. In addition, in the case of LLDPE and HDPE, annealed sheets were prepared by heating in an oven at 120 °C for 10 h, followed by slow cooling for two hours in the oven with the power off; these samples are designated LLDPE-a and HDPE-a. The samples to be used in the mass spectrometer apparatus were discs of diameter 50 mm cut from the centre of the films, with thicknesses in the range 0.74–0.96 mm measured with an electronic micrometer.

3.3. Single and mixed gases

The single gases and gas mixtures were obtained from BOC Ltd. The single gases were O_2, CO_2 and N_2, and were quoted as 99.7% pure. The mixtures of gases in the required concentrations were also obtained from BOC Ltd, with certified mixtures of about the same percentage purity. Following our previous study [4] the gas proportions (%) in mixtures will be expressed in the order O_2:CO_2:N_2.

3.4. Experimental apparatus and procedure

The transport properties were determined by the dynamic flow rate method [6]. The equipment consists of an input line and an output line, separated by a cell, where the samples in the form of a flat membrane were placed. After evacuating both gas lines, the absorption experiment starts when the test gas (single or mixed gas) is introduced at time $t=t_o$ at a known pressure to the input line, and the gas permeating through the sample to the output line is removed continuously, and a flow rate is recorded as a function of time. Eventually, equilibrium is reached when the flow rate becomes constant. The desorption experiment then takes place when the gas flux in question is shut off from the input line and evacuated by means of the Fore roughing pump (low vacuum side), and the flow rate is monitored continuously at the output line until the flow ceases. Thus, the transport properties D, P and hence S, can be determined from each experiment.

The single gases and different mixed gases were investigated with a quadrupole type mass spectrometer, Model DAQ-100. Further details of the mass spectrometer system were presented in previous publications [4,6].

A schematic representation of the mass spectrometer system can be seen in Fig. 1. The initial (boundary) conditions were achieved by evacuating the volume in contact with both sides of the sample (no. 5, from Fig. 1)

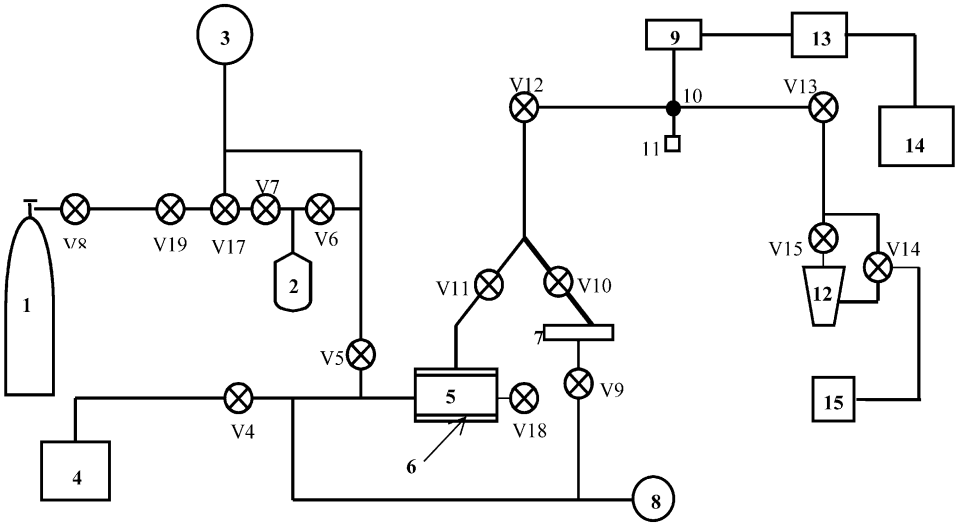

Fig. 1. A schematic representation of the mass spectrometer system. Symbols: *v*, valve; 1, gas cylinder; 2, gas reservoir; 3, Reservoir pressure gauge; 4, FORE roughing pump; 5, film sample cell; 6, heater; 7, pinhole cell (for calibration); 8, McLeod gauge; 9, Mass spectrometer head; 10, sensor; 11, Penning sensor; 12, Diffusion pump; 13, Spectramass console; 14, PC computer; and 15, Vacuum pump.

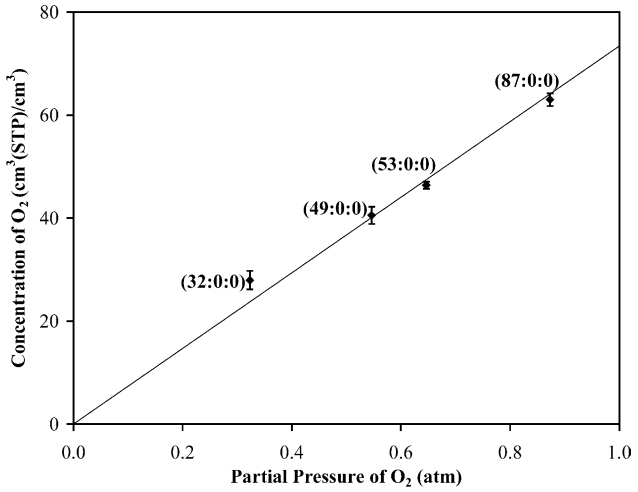

Fig. 2. Concentration of O_2 in LLDPE film vs. partial pressure of O_2. The temperature of the samples was 22–25 °C. The proportion of gases is O_2:CO_2:$N_{2\%}$.

using a Fore roughing pump (no. 4) and a vacuum pump (no. 15). The permeant gas was then introduced at a known pressure up to about 1050 mbar (measured by gauge no. 3) to one side of the sample (low vacuum side), passing through a gas reservoir (no. 2). The other side (high vacuum side) was continuously pumped with the vacuum pump (no. 15) to an ultimate vacuum of 2×10^{-8} Torr. The flux of the permeant gas emerging from the sample was measured by a quadrupole sensor (no. 10). The sensor is located in the pumping line between the diffusion pump (no. 12) and the sample cell (no. 5).

If the diffusion pump (no. 12) speed is great enough to ensure a constant pumping rate to the volume between it (no. 12) and the sample, the flux of gas through the volume will be proportional to the pressure of the gas at the head (no. 9, from Fig. 1).

The sample (no. 5) and pinhole (no. 7) cells are located between the high vacuum and low vacuum sides. With the operation of the two valves, (V10 and V11), one could either select the pinhole or the sample to be inserted between the high and low vacuum sides of the apparatus, the pinhole being introduced only for the purpose of calibration [6].

When the pinhole is interposed between the high (no. 15) and low (no. 4) vacuum sides, the number gas molecules striking unit area per second, N_g, is governed by Eq. (9).

$$N_g = 1/4\rho v \tag{9}$$

where ρ is the number density of the effusing gas, and v is the mean speed of the molecules. By applying simple gas laws, Eq. (9) can be written as follows (Eq. (10)).

$$E_a = \frac{p}{p_o}\sqrt{\frac{kT}{2\pi m}} \tag{10}$$

where E_a is the effusion rate (flux) of the gas through the pinhole (as volume at atmospheric pressure), per unit area of pinhole per second, p is the input pressure (measured by an Edwards Vacustat McLeod gauge), p_o is atmospheric pressure (760 Torr, 1023.25 mbar), T is the gas temperature, m is the mass of gas molecule and k is Boltzmann's constant. The apparatus was calibrated by plotting the mass spectrometer signal vs. the known flux through the pinhole for a range of pressures (p) from 0 to 0.5 Torr. Also E_a can be written as follows (Eq. (11))

$$E_a A_h = A\Delta F_\infty \tag{11}$$

A_h is the pinhole area, A is the sample area and, ΔF_∞ is the steady state flux when the sample is in place.

Permeability, P, derived from above equations becomes Eq. (12)

$$P = \Delta F_\infty l/(p_1 - p_2) \tag{12}$$

ΔF_∞ is the steady state flux, l is the sample thickness, p_1–p_2 is the partial pressure difference across the sample.

Both sides of the system were pumped until all permeants were completely desorbed. The absorption experiment started when the permeant gas or mixture at a known pressure was introduced to the sample from the reservoir at a known time. Data were collected from just before the introduction of the gas and ended when a steady state was reached. Then, the desorption experiment began by evacuating the gas from the sample, and data were collected from the end of the absorption until the steady state background levels were achieved again.

3.5. Data analysis

For the adsorption experiment, the diffusion coefficients were determined by fitting the flux versus time data to Eq. (5). The desorption experiment was carried out after steady-state had been achieved in the absorption run; the desorption data were fitted to Eq. (13). The parameters fitted in each experiment were the diffusion coefficient, D; the steady state flux, ΔF_∞; and the adsorption or desorption time of the gas, t.

$$\Delta F = 1 - \left[(4/\sqrt{\pi})X\sum_{i=1}^{\infty}\exp(-n_i^2X^2)\right]\Delta F_\infty \quad \text{for } n \text{ odd} \tag{13}$$

The permeability coefficients, P, were determined from Eq. (12).

The solubility coefficients, S, were then calculated from Eq. (8).

4. Results and discussion

4.1. Single gases

4.1.1. Solubility

The preliminary observation was that a linear correlation was found between gas concentration and partial pressure of

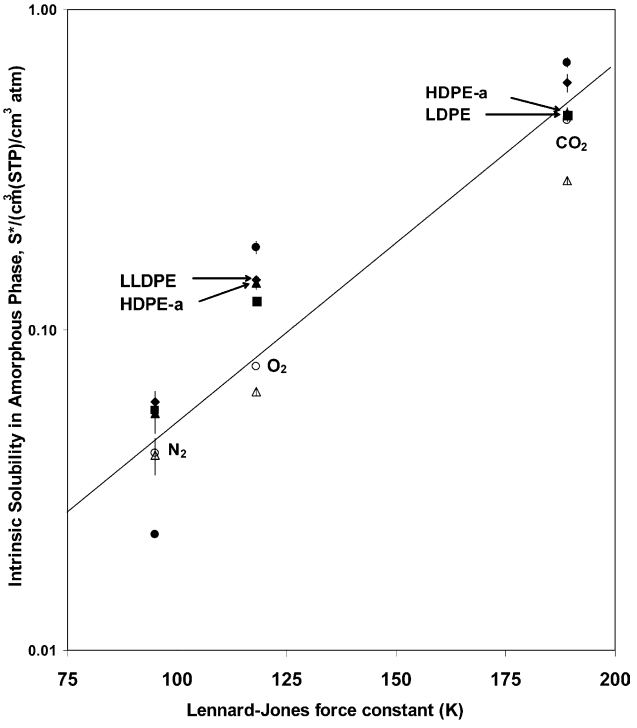

Fig. 3. Intrinsic solubility of pure gases in amorphous phase vs. Lennard–Jones force constant for LDPE, LLDPE, LLDPE-a, HDPE, and HDPE-a. The a refers to annealed samples. Symbols: ○, Michaels data for O_2, N_2 and CO_2; ●, O_2; ■, CO_2; and ▲, N_2. The full line is suggested by Eq. (14).

the single gases O_2, CO_2 or N_2, showing that Henry's law is obeyed to a good approximation in each case, see for example, Fig. 2.

The greater solubility of CO_2 compared with O_2 and N_2 may be attributed to the greater Lennard–Jones force constant. The solubility of non-polar gases is largely governed by the nature of the intermolecular forces within the gas, which can be quantified by the magnitude of the Lennard–Jones force constant. The gases which have the highest intermolecular forces and hence the highest Lennard–Jones constants, may be expected to have the greatest solubilities, on the basis that dissolving a gas in a polymer is similar to dissolving it in a liquid, because only the non-crystalline regions are accessible. It is therefore assumed that $S = V_a S^*$ where V_a is the amorphous volume fraction determined by DSC and S^* is the hypothetical solubility of completely amorphous polymer. Michaels and Bixler [7] used the work of Jolley and Hilderband [8] on solubility of gases, to correlate S^* to the Lennard–Jones force constant, $(\bar{\varepsilon}/k)$ of the gas. The equation of Michaels and Bixler [7] relating amorphous solubilities with a range of 12 gases within polyethylene, at 25 °C is given as

$$\ln S^* = 0.022\bar{\varepsilon}/k - 5.07 \quad (14)$$

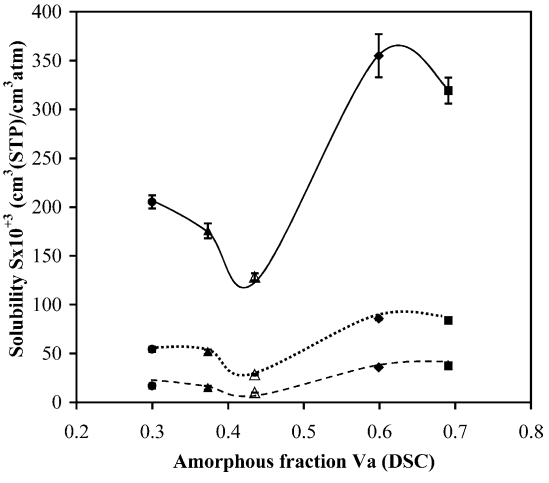

Fig. 4. Solubility vs. amorphous fraction for pure gases. ♦, LLDPE; ■, LDPE; ▲, HDPE-a; ●, LLDPE-a; Δ, HDPE; …, O_2; —, CO_2; and - -, N_2.

Table 3
Solubility (S) results at 22–25 °C

Samples	Amorphous fraction (%Va)	$S\times10^{+3}$/cm^3 (STP)/cm^3 atm		
		O_2	CO_2	N_2
LDPE	68	83.7±1.4	319.2±13.3	37.3±2.5
LLDPE	60	85.7±1.4	345.9±22.0	35.8±0.8
HDPE	44	29.0±0.8	128.0±3.7	10.1±0.1
HDPE-a	37	51.8±2.3	175.5±7.6	15.0±2.0
LLDPE-a	30	54.3±2.3	205.2±6.7	16.8±2.5

Data extracted from Tables 5–7.

Fig. 3 shows the collected results for the intrinsic solubilities versus the Lennard–Jones constant. Although there is general agreement between the present results and those of Michaels and Bixler [7] and more recently Holden et al. [9], there are significant deviations from a unique relationship between S^* and the Lennard–Jones constant which are well outside experimental error.

The five data points for each gas shown in Fig. 3, derive from our five polyethylene materials, and suggest that there can be different structures in the amorphous regions between different samples of polyethylene. The experimental uncertainties where not shown are smaller than the size of the symbols. Therefore, there is a structure effect on the solubility and permeability, probably due to the change in the distribution of the accessible free volume.

There is no obvious correlation between solubility and amorphous fraction in any material investigated (Fig. 4). The solubility for HDPE increases on annealing whereas the solubility for LLDPE decreases (Table 3). It appears therefore that the solubility is not simply related to the amorphous volume fraction, as supposed previously [7,9].

4.2. Diffusion and permeability

The higher diffusion for O_2 than CO_2 and N_2 in all our polyethylene samples (Table 4 and Fig. 5(a)) has also been found in other polymers such as PET [4,6,10,13], PVC [13], HDPE [10], oriented PE [11], other PE's [6,7,12–14] and many rubbers [6,13].

Table 4
Diffusion (D) results at 22–25 °C

Samples	Amorphous fraction (%Va)	$D\times10^{+7}$/cm^2/s		
		O_2	CO_2	N_2
LDPE	68	3.1±0.1	2.4±0.1	2.0±0.1
LLDPE	60	2.1±0.1	1.8±0.1	1.3±0.1
HDPE	44	1.9±0.1	1.3±0.1	1.1±0.1
HDPE-a	37	2.7±0.1	1.9±0.1	1.4±0.1
LLDPE-a	30	5.1±0.2	4.0±0.2	4.1±0.1

Data extracted from Tables 5–7.

The diffusion (Table 4 and Fig. 5(b)) and permeability (Tables 5–7) coefficients increase after annealing, despite the reduction in amorphous content. This has been observed by other authors [15,16]. The long time annealing may create free-volume holes of sufficient size in the amorphous regions to allow the gas molecules to diffuse more readily despite reducing the total amount of amorphous polymer.

4.3. Mixed gases

It is worth observing some interactions between the different gases depending on the structure of the polymers. For example, the solubility and permeability of N_2 is reduced considerably by the presence of CO_2 and/or O_2 in LDPE and HDPE-a, whereas they are decreased when CO_2 is present in LLDPE, see Table 7.

The solubility of O_2 is reduced in all materials by the presence of N_2, with the exception of LLDPE-a. The CO_2 also reduces the solubility of O_2 but only in annealed samples (HDPE-a and LLDPE-a), see Table 5.

The most prominent feature in our mixed gas results is the competition between O_2 and N_2 when they are present in mixtures, in materials with high amorphous fractions, LDPE and LLDPE. The major feature of the competition is that the permeability and solubility of O_2 are decreased when N_2 is

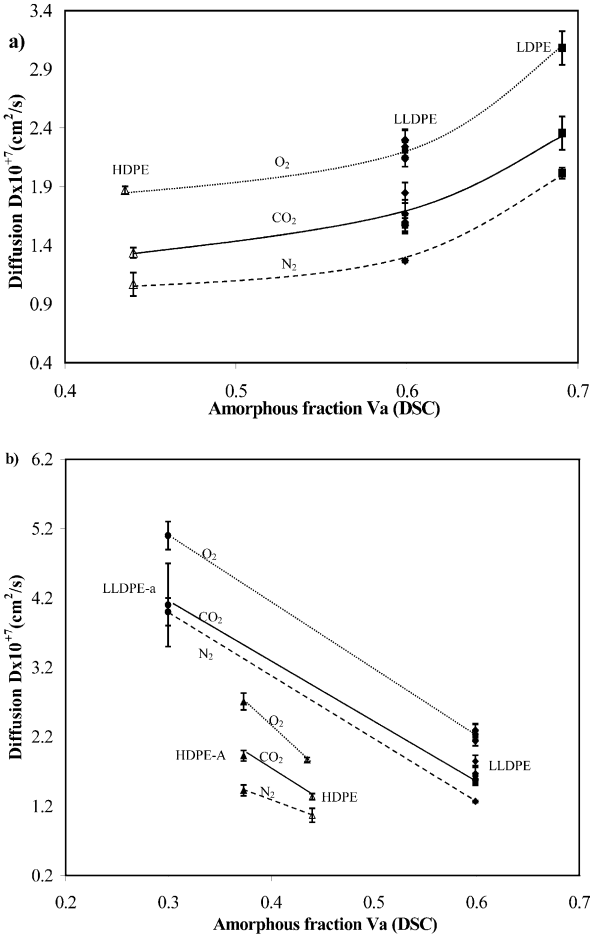

Fig. 5. (a) Diffusion of pure gases for non-annealed films vs. amorphous fraction. ♦, LLDPE; ■, LDPE; and Δ, HDPE. The lines as in Fig. 3. (b) Diffusion of pure gases for annealed and non-annealed films vs. amorphous fraction. ♦, LLDPE; ●, LLDPE-a; Δ, HDPE; and ▲, HDPE-a. The lines as in Fig. 4.

Table 5
Diffusion (D), solubility (S) and permeability (P) of O_2 in gas mixtures (O_2:CO_2:$N_{2\%}$) at 22–25 °C (Va: amorphous percentage—DSC)

Samples	%Va (DSC)	Gas mix (%)	Diffusion D ($D\times10^{+7}$/cm^2/s)	Solubility S ($S\times10^{+3}$/cm^3 (STP)/cm^3 atm)	Permeability P ($P\times10^{+10}$/cm^3 (STP)cm/cm^2 s cmHg)
LDPE	68	100:0:0	3.1±0.1	83.7±1.4	3.4±0.2
		50:0:50	3.1±0.1	68.0±3.1	2.7±0.1
		25:25:50	3.6±0.2	70.6±6.1	3.4±0.3
LLDPE	60	100:0:0	2.1±0.1	85.7±1.4	2.4±0.1
		50:0:50	2.2±0.1	74.0±2.7	2.1±0.1
		25:25:50	2.6±0.1	70.6±1.6	2.4±0.1
HDPE	44	100:0:0	1.9±0.1	29.0±0.8	0.7±0.1
HDPE-a	37	100:0:0	2.7±0.1	51.8±2.3	1.8±0.2
		50:0:50	2.6±0.1	38.4±3.8	1.3±0.1
		25:25:50	2.6±0.1	32.1±1.4	1.1±0.1
LLDPE-a	30	100:0:0	5.1±0.2	54.3±2.3	3.6±0.1
		50:0:50	4.7±0.2	53.6±2.8	3.3±0.1
		25:25:50	5.1±0.2	40.4±0.8	2.7±0.1

Note that $S=76\,P/D$ (cm^3 (STP)/cm^3 atm). The transport parameters units are given as: diffusion $D\times10^{+7}$/cm^2/s; solubility $S\times10^{+3}$/cm^3 (STP)/cm^3 atm; and permeability $P\times10^{+10}$/cm^3 (STP) cm/cm^2 s cmHg.

Table 6
Diffusion (D), solubility (S) and permeability (P) of CO_2 in gas mixtures (O_2:CO_2:$N_{2\%}$) at 22–25 °C (Va: amorphous percentage—DSC)

Samples	%Va (DSC)	Gas mix (%)	Diffusion D ($D\times10^{+7}$/cm^2/s)	Solubility S ($S\times10^{+3}$/cm^3 (STP)/cm^{3}atm)	Permeability P ($P\times10^{+10}$/cm^3(STP)cm/cm^2 s cmHg)
LDPE	68	0:100:0	2.4±0.1	319.2±13.3	9.9±0.3
		0:50:50	2.4±0.1	342.8±6.1	10.8±0.4
		25:25:50	2.6±0.2	319.6±17.4	10.8±0.7
LLDPE	60	0:100:0	1.9±0.1	354.9±22.0	8.6±0.1
		0:50:50	1.7±0.1	359.8±15.2	8.1±0.3
		25:25:50	1.8±0.1	313.8±13.1	7.1±0.4
HDPE	44	0:100:0	1.3±0.1	128.0±3.7	2.3±0.1
HDPE-a	37	0:100:0	1.9±0.1	175.4±7.6	4.4±0.1
		0:50:50	1.6±0.1	168.3±7.4	3.6±0.1
		25:25:50	1.7±0.1	175.1±5.0	4.0±0.1
LLDPE-a	30	0:100:0	4.0±0.2	205.2±6.7	10.7±0.3
		0:50:50	3.9±0.2	209.4±11.2	10.6±0.6
		25:25:50	3.9±0.1	205.7±13.4	10.5±0.5

Note that $S=76\ P/D$ (cm^3(STP)/cm^3 atm). The transport parameters units are given as: diffusion $D\times10^{+7}$/cm^2/s; solubility $S\times10^{+3}$/cm^3 (STP)/cm^3 atm; and permeability $P\times10^{+10}$/cm^3(STP)cm/cm^2 s cmHg.

present in the mixtures $50O_2$:$50N_{2\%}$. Another feature of the competition is that the permeability and solubility of CO_2 (Table 6) are increased by N_2 in the mixture $50CO_2$:$50N_{2\%}$ in LDPE, but they do not vary in the mixture $25O_2$:$25CO_2$:$50N_{2\%}$, where the ratio of N_2:O_2 is even higher. This suggests that the presence of O_2 can negate the effect of N_2.

The solubility and permeability of N_2 (Table 7) increase strongly in the presence of CO_2 in non-annealed LLDPE and decrease dramatically in LLDPE-a. No strong effect is seen in the other materials. The solubility, diffusion and permeability of CO_2 (Table 6) are independent of other gases, except in the case of LDPE as mentioned earlier.

In the LLDPE-a case, O_2 diffuses faster than the other gases present in the mixture (CO_2 and/or N_2) and may occupy some of the accessible sites in the polymer structure. While the occupation of the O_2 is occurring, CO_2 and N_2 start permeating the sample. Following that, CO_2 and N_2 may compete because of the fact that CO_2 dramatically reduces the diffusion and permeability of N_2. In this respect, the permeability and solubility of N_2 would be expected to decrease in materials with high crystallinity, such as LLDPE-a.

In the case of LLDPE, CO_2 increases the solubility and permeability of N_2. Lewis [4] also found that in PET, where the CO_2 swells the PET, it increases the diffusion and permeability of N_2. It is well known that CO_2 has a similar effect in other polymers [17].

From the solubility it is straightforward to calculate the number of gas molecules per unit volume at atmosphere

Table 7
Diffusion (D), solubility (S) and permeability (P) of N_2 in gas mixtures (O_2:CO_2:$N_{2\%}$) at 22–25 °C (Va: amorphous percentage—DSC)

Samples	%Va (DSC)	Gas mix (%)	Diffusion D ($D\times10^{+7}$/cm^2/s)	Solubility S ($S\times10^{+3}$/cm^3 (STP)/cm^{3}atm)	Permeability P ($P\times10^{+10}$/cm^3(STP)cm/cm^2 s cmHg)
LDPE	68	0:0:100	2.0±0.1	37.4±2.5	1.0±0.1
		50:0:50	2.0±0.1	33.8±1.6	0.9±0.1
		0:50:50	2.3±0.1	33.4±1.1	1.0±0.1
		25:25:50	2.3±0.2	35.8±3.4	1.1±0.1
LLDPE	60	0:0:100	1.3±0.1	35.8±0.8	0.6±0.1
		50:0:50	1.3±0.1	34.4±2.5	0.6±0.1
		0:50:50	1.6±0.1	50.2±0.1	1.0±0.1
		25:25:50	1.5±0.1	49.1±0.1	1.0±0.1
HDPE	44	0:0:100	1.1±0.1	10.1±0.1	0.1±0.1
HDPE-a	37	0:0:100	1.4±0.1	15.0±2.0	0.3±0.1
		50:0:50	1.7±0.1	18.5±0.4	0.4±0.1
		0:50:50	1.4±0.1	17.2±2.3	0.3±0.1
		25:25:50	1.5±0.1	17.6±0.1	0.4±0.1
LLDPE-a	30	0:0:100	4.1±1.0	16.8±2.5	0.9±0.1
		50:0:50	3.1±0.1	19.8±0.1	0.8±0.1
		0:50:50	3.7±0.1	5.0±0.2	0.2±0.1
		25:25:50	3.5±0.1	8.5±0.7	0.4±0.1

Note that $S=76\ P/D$ (cm^3 (STP)/cm^3 atm). The transport parameters units are given as: diffusion $D\times10^{+7}$/cm^2/s; solubility $S\times10^{+3}$/cm^3 (STP)/cm^3 atm; and permeability $P\times10^{+10}$/cm^3 (STP)cm/cm^2 s cmHg.

Table 8
Number of O_2, CO_2 or N_2 molecules per monomer of PE in the diffusion of pure gases. (Va: amorphous percentage—DSC)

Samples	Amorphous fraction %Va (DSC)	Number of gas molecules per polymer monomer (N g m)		
		N g m$\times 10^{+5}$/(gas molecule/monomer)		
		O_2	CO_2	N_2
LDPE	68	10.4±0.2	39.7±1.7	4.6±0.3
LLDPE	60	10.7±0.2	44.1±2.7	4.5±0.1
HDPE	44	3.5±0.1	16.0±0.5	1.3±0.1
HDPE-a	37	6.4±0.3	21.8±0.9	1.9±0.2
LLDPE-a	30	6.8±0.3	25.5±0.8	2.1±0.3

pressure and, hence, to calculate the number of gas molecules per monomer average separation between each gas molecule in the film.

Although the concentration of gas molecules is small considered in terms of gas molecule per monomer (Table 8), the average distance between gas molecules is relatively small (see Table 9(a) and (b)), suggesting a possible reason why interactions between molecules of different gases could occur.

5. Conclusions

For the solubilities of single gases, several straightforward conclusions are possible. First, for the comparatively low pressures studied, the solubilities for oxygen, nitrogen and carbon dioxide are linearly proportional to the gas pressure, i.e. Henry's law is obeyed. Secondly, there is a reasonable correlation between the solubilities and the Lennard–Jones force constants, as concluded by previous workers. Thirdly, the solubilities do not show clear correlations with the crystallinity as determined by DSC. Annealing can cause either a decrease or an increase in solubility depending on the chemical structure, although there is always an increase in density.

In the case of mixed gases, the solubility of one gas is generally affected by the presence of a second gas, with the exception of carbon dioxide where the solubility, diffusion and permeability are almost independent of the presence of other gases. The solubility and permeability of oxygen and nitrogen can be either increased or decreased by the presence of carbon dioxide, showing that these effects presumably depend on subtle details of the polymer morphology, so that no simple generalizations are possible.

The clearest effect which has been observed is the apparent competition between nitrogen and oxygen in terms of solubility. It is clear from all the results presented in this paper that a satisfactory understanding of the mechanisms of solubility and diffusion will require much further experimental study of the effects of polymer structure and morphology, in parallel with measurements of solubility and diffusion.

Table 9a
The shortest distance (nm) between each gas molecule in the polyethylene films for single gases (O_2, CO_2, or N_2) at 1 atm (Va: amorphous percentage—DSC)

Samples	Amorphous fraction (%Va)	The shortest distance between each gas molecule in PE films (nm)		
		O_2	CO_2	N_2
LDPE	68	7.6±0.1	4.9±0.2	10.0±0.7
LLDPE	60	7.6±0.1	4.7±0.3	10.1±0.2
HDPE	44	10.9±0.3	6.6±0.2	15.5±0.1
HDPE-a	37	9.0±0.4	6.0±0.3	13.5±1.8
LLDPE-a	30	8.8±0.4	5.7±0.2	13.0±1.9

Table 9b
The shortest distance (nm) between gas molecules in the polyethylene films for mixed gases (O_2:CO_2:N_2) at 1 atm (Va: amorphous percentage—DSC)

Samples	(% Va)	Gas mix (%)	The shortest distance between mixed gas molecules in PE films (nm)
LDPE	68	50:0:50	7.1
		0:50:50	4.6
		25:25:50	4.4
LLDPE	60	50:0:50	7.0
		0:50:50	4.5
		25:25:50	4.4
HDPE-a	37	50:0:50	8.7
		0:50:50	5.9
		25:25:50	5.5
LLDPE-a	30	50:0:50	8.0
		0:50:50	5.6
		25:25:50	5.3

Acknowledgements

This research was funded by the White Rose Faraday Packaging Partnership and EPSRC. We thank the BP Chemicals, MCI Japan for providing suitable films and polymer granules, and Crown Cork as the industrial collaborators.

References

[1] Hofman D, Ulbrich J, Fritsch D, Paul D. Polymer 1996;37:4773–85.
[2] Kamaruddin HD, Koros WJ. J Membr Sci 1997;135:147–59.
[3] Shilton SJ, Bell G. Polymer 1996;37(3):485–92.
[4] Lewis ELV, Duckett RA, Ward IM, Fairclough JPA, Ryan AJ. Polymer 2003;44:1631–40.
[5] Auras R, Harte B, Selke S. School of Packaging, MSU, East Lansing, MI, US, pp. 1011–21, 2002.
[6] Webb JA, Bower DI, Ward IM, Cardew PT. J Polym Sci, Part B: Polym Phys 1993;31:743–57.
[7] Michaels AS, Bixler HJ. J Polym Sci 1961;50:393–412.
[8] Jolley JE, Hilderband HJ. J Am Chem Soc 1958;80:1050.
[9] Holden PS, Orchard GAJ, Ward IM. J Polym Sci, Polym Phys Ed 1985;23:709–31. pp. 2295–306.
[10] Michaels AS, Vieth WR, Barrie JA. J Appl Phys 1963;34:13–20.

[11] Norenberg H, Miyamoto T, Fukugami N, Tsukahara Y, Smith GD, Briggs GAD. Vacuum 1999;53:313.
[12] Michaels AS, Vieth WR, Barrie JA. J Appl Phys 1963;43:1–12.
[13] Paul DR, DiBenedetto AT. J Polym Sci, Part C 1965;10:17.
[14] Crank J, Park GS. Diffusion in polymers. London: Academic Press; 1968.
[15] Campan V, Lopez ML, Andrio A, Riande E. Macromolecules 1998; 31:6984–90.
[16] Villaluenga JPG, Seoane B. Polymer 1998;39:3655.
[17] Chiou JS, Barlow JW, Paul DR. J Appl Polym Sci 1985;30:2633.